9-2015

Nanoscale Alloying in Electrocatalysts

Shiyao Shan

Jinfang F. Wu

Ning Kang

Hannah Cronk

Yinguang G. Zhao

See next page for additional authors

Catalysts **2015**, *5*, 1465-1478; doi:10.3390/catal5031465

OPEN ACCESS

catalysts

ISSN 2073-4344

www.mdpi.com/journal/catalysts

Review

Nanoscale Alloying in Electrocatalysts

Shiyao Shan, Jinfang Wu, Ning Kang, Hannah Cronk, Yinguang Zhao, Wei Zhao, Zakiya Skeete, Pharrah Joseph, Bryan Trimm, Jin Luo and Chuan-Jian Zhong *

Department of Chemistry, State University of New York at Binghamton, Binghamton, NY 13902, USA;
E-Mails: sshan2@binghamton.edu (S.S.); jinwu@binghamton.edu (J.W.);
nkang3@binghamton.edu (N.K.); hcronk1@binghamton.edu (H.C.);
yzhao58@binghamton.edu (Y.Z.); wzhao15@binghamton.edu (W.Z.);
zskeete1@binghamton.edu (Z.S.); pjoseph2@binghamton.edu (P.J.);
btrimm1@binghamton.edu (B.T.); jluo@binghamton.edu (J.L.)

* Author to whom correspondence should be addressed; E-Mail: cjzhong@binghamton.edu;
Tel.: +1-607-777-4605.

Academic Editor: Minhua Shao

Received: 16 May 2015 / Accepted: 5 August 2015 / Published: 19 August 2015

Abstract: In electrochemical energy conversion and storage, existing catalysts often contain a high percentage of noble metals such as Pt and Pd. In order to develop low-cost electrocatalysts, one of the effective strategies involves alloying noble metals with other transition metals. This strategy promises not only significant reduction of noble metals but also the tunability for enhanced catalytic activity and stability in comparison with conventional catalysts. In this report, some of the recent approaches to developing alloy catalysts for electrocatalytic oxygen reduction reaction in fuel cells will be highlighted. Selected examples will be also discussed to highlight insights into the structural and electrocatalytic properties of nanoalloy catalysts, which have implications for the design of low-cost, active, and durable catalysts for electrochemical energy production and conversion reactions.

Keywords: nanoalloys; electrocatalysts; oxygen reduction reaction; phase structure; alloying degree; electrocatalytic activity

---

1. Introduction

The design of active, stable and low-cost catalysts is essential for many reactions in electrochemical energy production, conversion and storage. Metal nanoparticles, especially alloy nanoparticles, have attracted a great deal of interest in both experimental and theoretical studies [1–3]. It is the nanoscale size range over which metal nanoparticles undergo a transition from metallic to atomic properties which leads to unique electronic and catalytic properties different from their bulk counterparts. Significant advances have been made in harnessing the nanoscale catalytic properties in energy and environmental fronts [3]. However, challenges remain, especially in preparation and characterization of active, robust, low-cost nanocatalysts with controllable sizes, shapes, compositions and structures.

An alloy is a mixture of two or more metallic species, which can exist either in a complete solid solution state exhibiting a single phase characteristics or in a partial or phase-segregated solid solution state with multiple phases. Nanoalloy (NA) differs from bulk alloys in several significant aspects in terms of mixing patterns and geometric shapes. There are different types of mixing patterns, two of which include completely phase segregated NAs where the different phases share either an extended mixed interface or a very limited number of hetero-nuclear metal bonds, and mixed NAs with chemically ordered/disordered structures. The degree of segregation, mixing and atomic ordering depends on a number of factors, including relative strengths of differences in atomic sizes, surface energies of the component element, homoatomic *vs.* heteroatomic bonds, charge transfer between the different atomic species, and strength of binding to surface ligands or support materials. The observed atomic arrangement for a particular alloy depends critically on the balance of the preparation and usage conditions. By alloying, changes including atomic structure, physical and optical properties, and chemical properties could lead to two major effects: (i) ensemble effect where hetero-nuclear metals geometrically arranged in the favor of certain properties (e.g., catalytic process); (ii) ligand effect where electronic charge transfer between hetero-nuclear metals induces the change of functionality of metals (e.g., molecule adsorption properties) [4]. It is noted that the change of geometric arrangement by varying alloy composition or structural ordering/disordering cannot be done without changing electronic atmosphere. In catalysis, alloying hetero-nuclear metals plays a role in several different aspects, including (i) activation of the main components for enhanced activity; (ii) activation of successive reaction for the enhancement of overall reactions; (iii) removal of poisonous intermediates to facilitate the reactions; (iv) inhibition of certain intermediates and byproducts; and (v) reactants storage.[5] In addition, the surface structures of NAs could be very complex due to the enrichment of certain element in the core or shell. In the case of metal dissolution ("dealloying") in the presence of acidic electrolytes, often referred to as Pt-skin structure formation [6,7], the details of the noble metal skin could be influenced strongly by the structural types of the NAs, the understanding of which in terms of structural evolution, noble metal skin or d-band center shift has attracted increasing interests in electrocatalysis.

Supported metal nanoparticles from traditional preparative methods have been well demonstrated for various catalytic reactions [2,3,8]. In the last decade, new approaches to the synthesis of molecularly capped metal nanoparticles for the preparation of catalysts have been rapidly emerging (see Figure 1). While some of the catalysts exploit the functional groups from the capping shell of the nanoparticles, most others explore the surface active sites over the metal nanoparticles either after removing the capping layers [9] or through open channels of the capping layers [10]. In addition, the nanoscale facet is an

important factor in catalysis. For noble metal (e.g., Pt, Pd) alloyed with other transitions metals (e.g., Ni, Cu, Co, *etc.*), a volcano curve has been observed for certain metal ratios (e.g., 1:1, 1:3, or 3:1) in binary nanocatalysts [2]. Besides various nanostructural design parameters [11], the understanding of how these factors play an important role on catalytic properties is increasingly important.

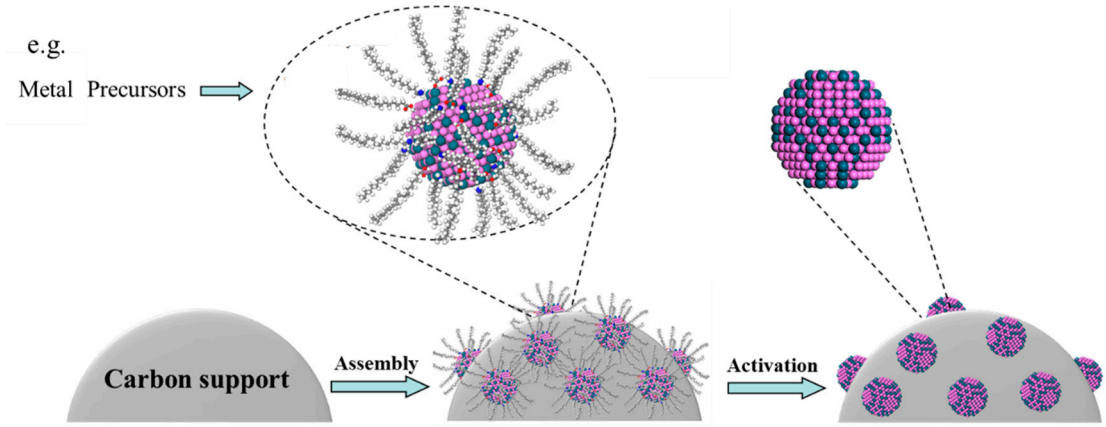

Figure 1. Illustration of the synthesis, assembly, and activation of nanoalloy particles for the preparation of the supported electrocatalysts.

In this article, some of the recent findings in the exploration of nanoscale alloying degree for the preparation of the supported nanoalloy catalysts for catalytic and electrocatalytic reactions [12–17] will be highlighted. One important focus is the understanding of the structural correlation of nanoscale alloying properties with the electrocatalytic properties.

2. Synthesis and Preparation

The synthesis of molecularly-capped metal nanoparticles as building blocks for engineering the nanoscale catalytic materials takes advantage of diverse attributes, including monodispersity, processability, and stability in terms of size, shape, composition, phase and surface properties in comparison with traditional approaches [18]. One important approach involves core-shell type synthesis [19]. The core and shell are from different matters in close interaction, including inorganic/organic and inorganic/inorganic combinations [20,21]. The synthesis of metal nanoparticles in the presence of organic capping agents to form encapsulated metal nanoparticles has demonstrated promises for preparing nanocatalysts [20,21]. The coupling of molecularly-mediated synthesis of nanoparticles and post-synthesis thermochemical processing under controlled temperatures and atmospheres have demonstrated effectiveness in the preparation of nanocatalysts. In comparison with other methods such as plasmatic cleaning or chemical cleaning [22], thermochemical processing strategy is not only effective in removing the encapsulation, but also in refining the nanostructural parameters. The combination of the molecular encapsulation based synthesis and thermochemical processing strategies typically involves a sequence of steps for the preparation of nanoalloy catalysts: (1) chemical synthesis of the metal nanocrystal cores capped with ligands, (2) assembly of the encapsulated nanoparticles on supporting materials (e.g., carbon powders, TiO_2 or SiO_2), and (3) thermal treatment of the supported nanoparticles [12–17]. The size and composition of the nanoparticles produced by thermochemical processing are controllable. As shown for a series of binary and ternary alloy

nanoparticle systems in Table 1 [12–17,23–35], the catalysts prepared by the molecularly-mediated synthesis and thermochemical processing methods have demonstrated enhanced catalytic and electrocatalytic properties for oxygen reduction reaction (ORR), methanol oxidation reaction (MOR), and ethanol oxidation reaction (EOR), *etc.*

Table 1. Examples of alloy nanoparticles and catalysts prepared by molecularly-mediated synthesis and thermochemical processing methods.

Catalysts	Synthesis method	Catalytic reactions	Refs
	Bimetallic nanoalloys		
PtNi NPs (2–8 nm)/C, TiO_2, or SiO_2	*Precursor*: $Pt(acac)_2$, $Ni(acac)_2$; *Capping agent*: oleic acid (OA), oleylamine (OAM); *Reducing agent*: 1,2-hexadecanediol (HDD); *Solvent*: octyl ether (OE)	ORR, CO oxidation	[12,23]
PtCo NPs (2–8 nm)/C, TiO_2 or SiO_2	*Precursor*: $Pt(acac)_2$, $Co_2(CO)_8$; *Capping agent*: oleic acid and oleylamine; *Reducing agent*: 1,2-hexadecanediol; *Solvent*: octyl ether	ORR, CO oxidation	[12,23]
PtRu (~5 nm)/C	*Precursor*: $Pt(acac)_2$, $Ru(acac)_2$; *Capping agent*: oleic acid and oleylamine; *Reducing agent*: 1,2-hexadecanediol; *Solvent*: octyl ether	EOR, CO oxidation	[24]
AuCu (~5 nm)/C, SiO_2	*Precursor*: $HAuCl_4$, $CuCl_2$; *Capping agent*: 1-decanethiol (DT); Tetraoctylammonium bromide (TOABr); *Reducing agent*: $NaBH_4$; *Solvent*: H_2O and Toluene	CO oxidation	[14]
AuCu (4–8 nm)/C	*Precursor:* Au NPs and Cu NPs; *Capping agent*: 1-decanethiol (DT); Tetraoctylammonium bromide (TOABr); *Method*: Thermally aggregated growth	CO oxidation	[14]
PdNi (7–10 nm)/C	*Precursor*: $Pd(acac)_2$, $Ni(acac)_2$; *Capping agent*: oleic acid and oleylamine; *Reducing agent*: 1,2-hexadecanediol; *Solvent*: octyl ether or benzyl ether	ORR, CO oxidation	[25]
PdCu (7–10 nm)/C	*Precursor*: $Pd(acac)_2$, $Cu(acac)_2$; *Capping agent*: oleic acid and oleylamine; *Reducing agent*: 1,2-hexadecanediol; *Solvent*: octyl ether or benzyl ether	EOR, CO oxidation	[26]
AuPt (~4–5 nm)/C	*Precursor*: $HAuCl_4$, $HPtCl_4$; *Capping agent*: DT, OAM/OA; *Reducing agent*: $NaBH_4$; *Solvent*: H_2O and Toluene;	ORR, MOR	[13,27,28]

Table 1. *Cont.*

Catalysts	Synthesis method	Catalytic reactions	Refs
	Trimetallic Nanoalloys		
PtNiCo (3–5 nm)/C, TiO_2, and SiO_2	*Precursor*: $Pt(acac)_2$, $Ni(acac)_2$, $Co(acac)_3$; *Capping agent*: oleic acid and oleylamine; *Reducing agent*: 1,2-hexadecanediol; *Solvent*: octyl ether	ORR, CO oxidation	[12,29,30]
PtVCo (3–5 nm)/C	*Precursor*: $Pt(acac)_2$, $VO(acac)_2$, $Co(acac)_3$; *Capping agent*: oleic acid and oleylamine; *Reducing agent*: 1,2-hexadecanediol; *Solvent*: octyl ether	ORR, CO oxidation	[17,31]
PtNiFe (3–5 nm)/C	*Precursor*: $Pt(acac)_2$, $Ni(acac)_2$, $Fe(CO)_5$; *Capping agent*: oleic acid and oleylamine; *Reducing agent*: 1,2-hexadecanediol; *Solvent*: octyl ether	ORR, CO oxidation	[32,33]
PtIrCo (3–5 nm)/C	*Precursor*: $Pt(acac)_2$, $Ir_4(CO)_{12}$, $Co(acac)_2$; *Capping agent*: oleic acid and oleylamine; *Reducing agent*: 1,2-hexadecanediol; *Solvent*: octyl ether	ORR, CO oxidation	[15,17,34]
PtVFe (3–5 nm)/C	*Precursor*: $Pt(acac)_2$, $VO(acac)_2$, $Fe(CO)_5$; *Capping agent*: oleic acid and oleylamine; *Reducing agent*: 1,2-hexadecanediol; *Solvent*: octyl ether	ORR,	[35,36]

3. Examples of Nanoalloy Electrocatalysts

Pt- or Pd-based nanoalloys have been extensively explored as electrocatalysts for electrocatalytic ORR, which is an important reaction in proton exchange membrane fuel cell (PEMFC), an electrochemical energy conversion device that converts hydrogen at the anode and oxygen at the cathode through a membrane electrode assembly (MEA) into water and produce electricity. The desired reaction pathway in the cathode of a PEMFC is $4e^-$ reduction reaction of oxygen. During PEMFC reaction process, the voltage is the summation of the thermodynamic potential E_{Nernst}, the activation overpotential η_{act} (from both anode and cathode overpotentials, *i.e.*, $\eta_{act(\text{cathode})} - \eta_{act(\text{anode})}$), and the ohmic overpotential η_{ohmic}. The thermodynamic potential is governed by Nernst equation in terms of the E_0 (1.23 V) and the operating concentrations ($P(H_2)$ and $P(O_2)$), the activation overpotential is dependent on the electrode kinetics in terms of current flow, and the overpotential associated with catalyst activity ($\eta_{act(catalyst)}$). The overpotential $\eta_{act(catalyst)}$ is large mainly attributed to the sluggish activity of ORR. The adsorption of O_2 over Pt surface could produce Pt–O or Pt–OH in a dissociative adsorption, which constitutes a four-electron reduction pathway forming water, or $Pt–O_2^-$ or $Pt–O_2H$ in an associative adsorption which often proceeds in a two-electron reduction pathway forming hydrogen peroxide. Although the understandings based on Pt skin on an alloy or dealloyed surface can explain partially some of the experimental facts, the exploration of how Pt–O or –OH intermediate species would influence the overall ORR by varying their binding strength and the formation and removal of Pt–O/Pt–OH species are known to play a key role in the overall electrocatalytic ORR over Pt-alloy catalysts [37]. The rational design of

Pt-alloys involving transition metals (M/M′) could create a bifunctional (or multifunctional) synergy for the formation and removal of Pt–O or Pt–OH species. For ternary catalysts, the introduction of a second M′ into Pt-M alloy may further lead to a manipulation of the surface oxophilicity by maneuvering –O/–OH species over M and M′ sites through structural or compositional manipulation [12,15,17,28–34]. The understanding of how Pt–OH and Pt–O binding energies can be tuned by the M/M′ oxophilicity would aid the design of the alloying metals for synergistic formation and removal of Pt–OH species in correlation with the structural and chemical complexity of the nanoalloys.

3.1. Bimetallic Nanoalloy Catalysts

Bimetallic nanoalloy catalysts derived from combinations of two heterometals often exhibit unique bifunctional or other physical and chemical properties. A strong correlation between the size, structure and catalytic activities was revealed over several interesting systems, e.g., PtNi, PtCo and AuPt [12,13,23,27,28]. Gold-platinum (AuPt) nanoalloys serve as an intriguing system in terms of the unique synergistic properties [12,27,28]. In contrast to the bulk counterpart which displays a miscibility gap at 20%–90% Au, nanoscale AuPt particles synthesized by wet chemical methods has shown alloy properties. The morphology and alloy structures are controllable, as shown by the example of $Au_{22}Pt_{78}$ nanoparticles on carbon support (Figure 2A). The observation of the indicated lattice fringes, 0.235 nm, corresponding to 111 planes, indicates that the carbon-supported nanoparticles are highly crystalline. Carbon-supported AuPt nanoparticles have been shown to exhibit alloying characteristics and possess a uniform distribution of the two metals across the entire nanoparticles. The subtle increase of the particle sizes for the thermochemcally-treated carbon-supported $Au_{22}Pt_{78}$ nanoparticles was due to the thermal sintering of the nanoparticles.

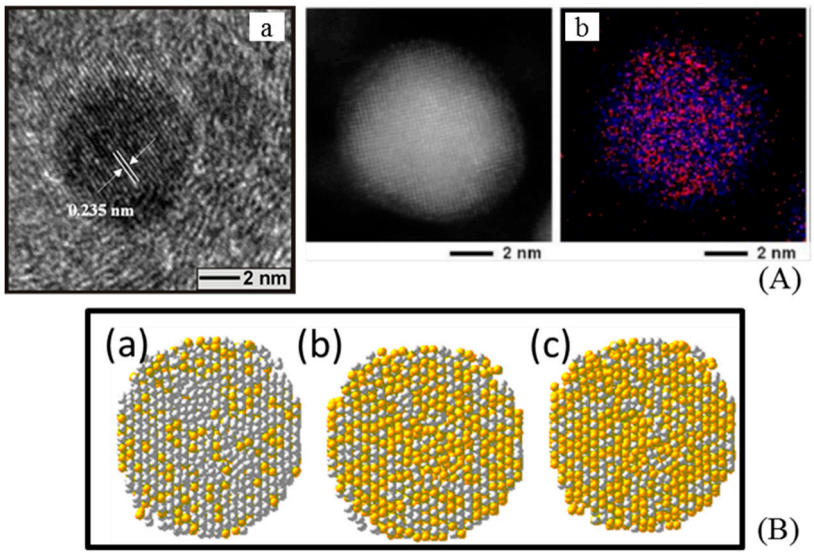

Figure 2. (**A**) HRTEM (a) and EDS (b) composition mapping for $Au_{22}Pt_{78}$/C (red: Pt, Blue: Au) nanoparticles; (**B**) Cross sections of 5.1 nm Pt-Au particles (about 5000 atoms) with random alloy structure: (**a**) $Pt_{77}Au_{33}$; (**b**) $Pt_{51}Au_{49}$ and (**c**) $Pt_{40}Au_{60}$.Pt atoms are in gray, Au in yellow. ((**B**) reproduced from reference [13] with permission. Copyright 2012, American Chemical Society; (**A**) reproduced from reference [27] with permission. Copyright 2010, American Chemical Society).

The detailed nanoscale alloying characteristics is recently evidenced by studies using element-specific resonant high energy X-ray diffraction coupled to pair distribution function analysis (HE-XRD/PDF) [12]. This technique, aided by Reverse Monte Carlo simulation (RMC) modeling, has provided an atomic-scale insight into the alloy structures of AuPt nanoparticles (Figure 2B). Pure Au and Pt nanoparticles are used to produce model configurations for Au_nPt_{100-n} nanoparticles (n = 40, 51, 77) where Au and Pt atoms show various patterns of chemical order-disorder effects. From the modeling, it was found that the alloying of Pt and Au occurs not only within a wide range of Pt-Au concentrations but is also stable in nanoparticles of different sizes.

The electrocatalytic ORR activities of AuPt nanoalloys have been assessed by rotating disk electrode (RDE) measurements [27]. As shown by RDE curves in Figure 3 for $Au_{22}Pt_{78}$/C and $Au_{49}Pt_{51}$/C catalysts, there are clear differences of the reduction currents in the kinetic region (0.8–0.9 V *vs.* NHE). These differences demonstrated that both the bimetallic composition and the phase structures had profound effects on the electrocatalytic activity. It is evident that the mass activity depends on both thermal treatment temperature and condition (Figure 3 insert). The data for $Au_{22}Pt_{78}$/C showed an increase of mass activity to a maximum at 400 °C and further decrease with increasing temperature. The decrease of the activity with temperature is consistent with the findings of the increased phase segregation and the Pt core-Au shell formation by experimental HRXRD/PDF data. The temperature for the maximum activity was also found to depend on the bimetallic composition, as supported by the observations of a maximum activity at 400 °C for $Au_{22}Pt_{78}$/C and a maximum activity at 600–700 °C for $Au_{49}Pt_{51}$/C. A combination of lattice parameter and surface structural effects as a result of the differences in composition and treatment conditions is believed to be operative. The observed differences between $Au_{22}Pt_{78}$/C and $Au_{49}Pt_{51}$/C catalysts indicate that there exists an optimized surface structure with an appropriate Pt–O bonding strength for achieving the enhanced electrocatalytic activity.

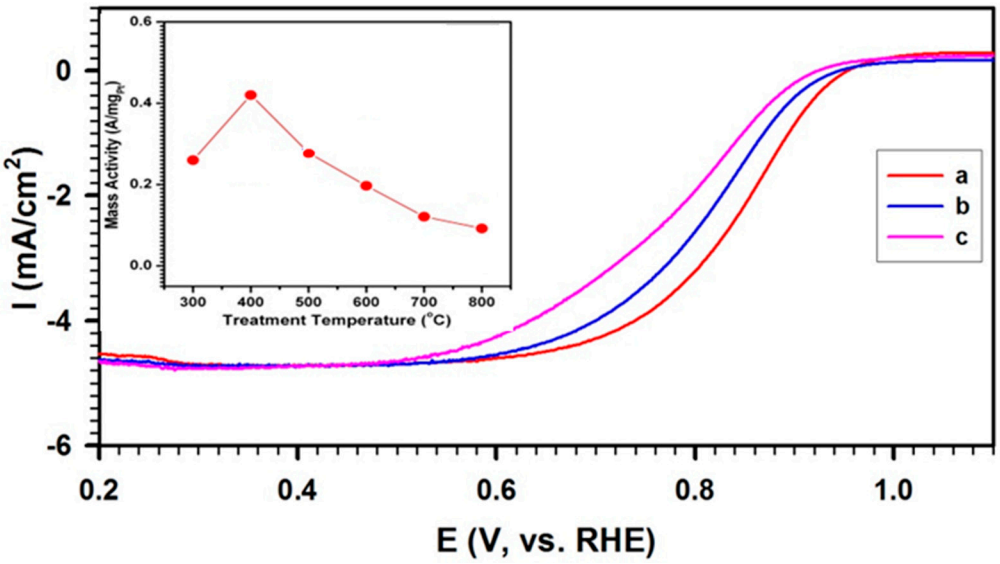

(A)

Figure 3. *Cont.*

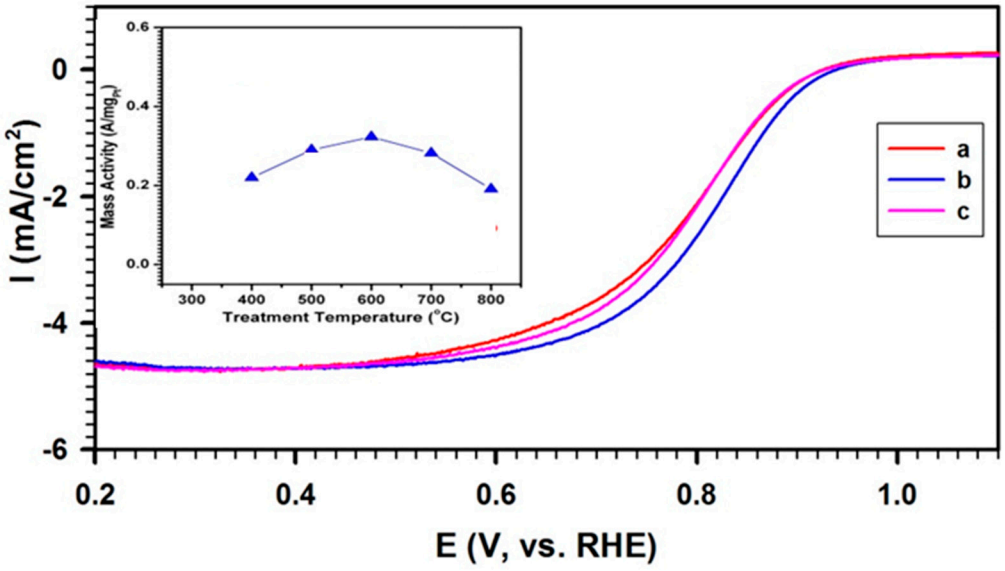

(**B**)

Figure 3. RDE curves for ORR for $Au_{22}Pt_{78}$/C (**A**) and $Au_{49}Pt_{51}$/C (**B**) catalysts treated under H_2 for 30 min (normalized for comparison) at 400 (**a**), 600 (**b**), and 800 °C (**c**). (Glassy carbon electrode (0.196 cm^2); 0.5 M H_2SO_4 saturated with O_2; catalyst loading: 10 μg; scan rate: 10 mV/s; speed: 1600 rpm). (reproduced from reference [27] with permission. Copyright 2010, American Chemical Society).

3.2. Trimetallic Nanoalloy Catalysts

In comparison with bimetallic systems, ternary nanoalloy catalysts provide an increased degree of structural tunability. In addition to the obvious tunability in nanoscale alloying, the manipulation of surface oxophilicity is demonstrated by the introduction of a second metal M′ into Pt-M alloys. In many cases, ternary Pt*MM*′ catalysts, where *M*, *M*′ = Ni, Co, Fe, V, Ir, *etc.*, have demonstrated enhanced electrocatalytic activities and stabilities in comparison with commercial Pt/C and their binary counterparts [12,15,17,29–36]. These aspects can be illustrated by studies of the ternary nanoalloy of PtIrCo in comparison with its binary counterparts [15,34]. As an example, the $Pt_{25}Ir_{20}Co_{55}$ nanoalloys prepared by the molecularly-mediated synthesis display a size of 2.5 ± 0.2 nm (Figure 4A). Based on HE-XRD/PDF characterization of PtIrCo/C and its binary counterparts (PtIr/C and PtCo/C) treated under H_2 at 400 and 800 °C, the detailed structural ordering and atomic configuration in the nanoparticles can modelled by RMC simulation (Figure 4B). Each of the configurations have the real stoichiometry and size of the nanoalloy and atomic PDFs computed from the configurations match the experimental PDF data very well.

$Pt_{45}Ir_{55}$ catalyst treated at 400 °C is a random alloy of Pt and Ir whereas that at 800 °C tends to segregate into a Ir-core and Pt-surface-enriched structure. This finding is qualitatively in agreement with the XPS based analysis of the relative surface composition, which showed a 16% increase in Pt upon treatment at 800 °C. $Pt_{73}Co_{27}$ catalyst treated at 400 °C features an alloy where Co atoms show some preference to the center of the nanoparticles whereas that at 800 °C, features an alloy with Co atoms being somewhat closer to the surface of the particle. In comparison, the $Pt_{25}Ir_{20}Co_{55}$ catalyst treated at 400 °C features an alloy where Co and Ir species tend to occupy the inner part of the nanoparticles while

Pt atoms show some preference to the surface of the nanoparticles. The ternary catalyst treated at 800 °C features a rather random type of alloy where Co, Pt and Ir atoms are almost uniformly distributed across the nanoparticles, a finding that was qualitatively in agreement with the small changes derived from the XPS analysis of the relative surface composition. These results reveal that the atomic distribution across the nanoparticles depends strongly on the binary/ternary composition and the thermochemical treatment temperature.

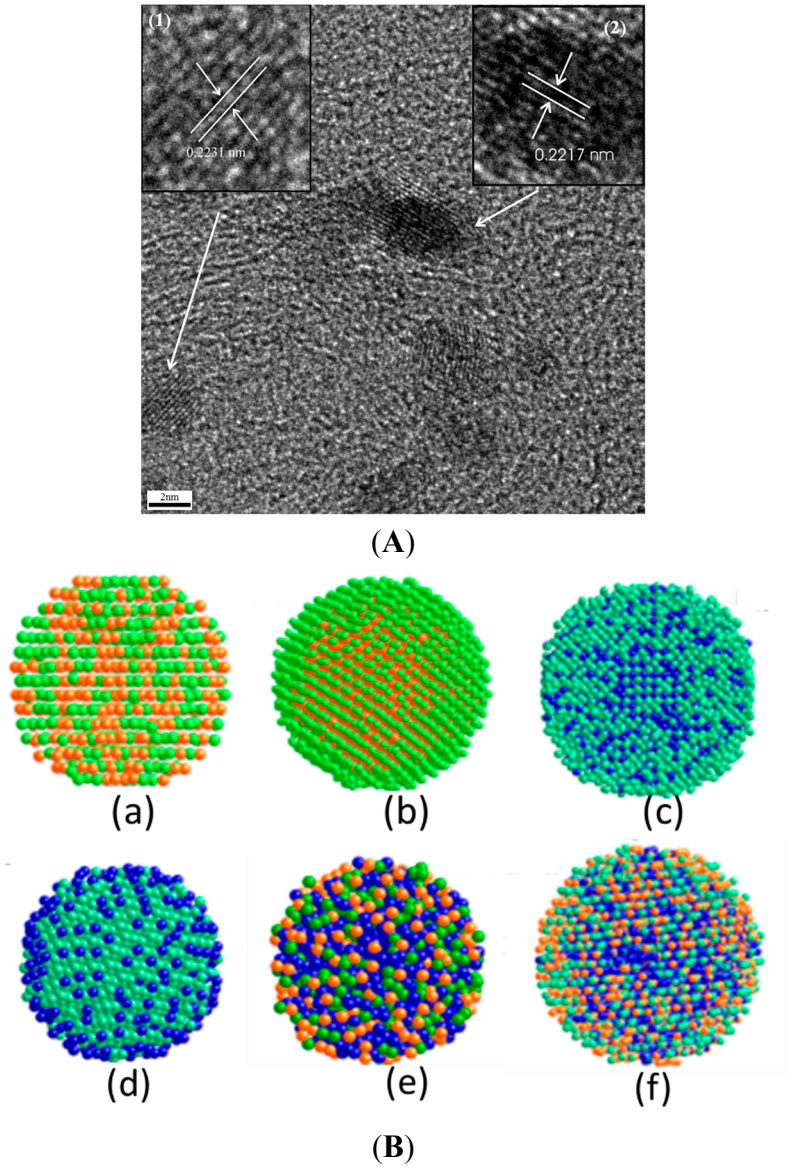

Figure 4. (**A**) HR-TEM for $Pt_{25}Ir_{20}Co_{55}$ and (**B**) RMC constructed models for $Pt_{45}Ir_{55}$, $Pt_{73}Co_{27}$, and $Pt_{25}Ir_{20}Co_{55}$ processed at 400 °C (**a**, **c**, **e**, respectively) and 800 °C (**b**, **d**, **f**, respectively). (Pt atoms: green, Ir atoms: orange, and Co atoms: blue). Note that the sizes of atoms are drawn not to scale to fit in the picture frame. ((**A**) reproduced from reference [15] with permission. Copyright 2013, American Chemical Society, (**B**) reproduced from reference [34] with permission. Copyright 2012, American Chemical Society).

The electrocatalytic activities of PtIrCo catalysts with different compositions for ORR were measured using the RDE method (e.g., $Pt_{65}Ir_{11}Co_{24}$/C(a), $Pt_{40}Ir_{28}Co_{32}$/C(b), and $Pt_{25}Ir_{20}Co_{55}$/C(c)). In comparison

with the mass activity for Pt/C catalysts, the mass activity was increased by a factor of 2–4 for these catalysts. There is a clear trend showing the increase of the mass activity with the increase of Co% and the decrease of Pt% in the nanoparticles. In comparison with the specific activity for Pt/C catalysts, the specific activity was increased by a factor of ~3 for the ternary catalysts. In comparison with its binary counterparts (PtCo and PtIr), the mass activity for $Pt_{25}Ir_{20}Co_{55}$/C nanocatalyst showed an increase by factor of ~2 (Figure 5A) [15]. Based on the detailed atomic structural data, the substantially shorter metal-metal distances in the ternary nanocatalysts are believed to be one of the key factors responsible for the improved catalytic properties. The increase in SA from lower to higher temperature (e.g., from 400 °C to 800 °C) for the ternary nanoalloys is also likely due to the further decrease in the metal-metal distances and the changes in coordination numbers. In addition to a favorable change in Co-Pt first coordination number, there are also changes in Co-Ir, Pt-Ir and Ir-Ir coordination numbers indicating an increased degree of alloying. Moreover, the introduction of Ir in PtCo to form a ternary system was indeed shown to increase stability of the electrocatalytic activity indicating the important role of the addition of Ir. The mass activity is the highest for the ternary catalyst among the three catalysts (see Figure 5A insert). The 2× increase of specific activity for the ternary catalyst in comparison with the relatively small increase for PtIr indicates the importance of adding a third metal with greater oxophilicity to the alloy. The marked enhancement of the activity ternary nanoparticles is believed to be linked to the decrease in the 1st Metal-Metal distances and the formation of alloy featuring either an Co-Ir core with Pt rich surface or a uniform distribution of Co, Pt and Ir species across the entire nanoparticle.

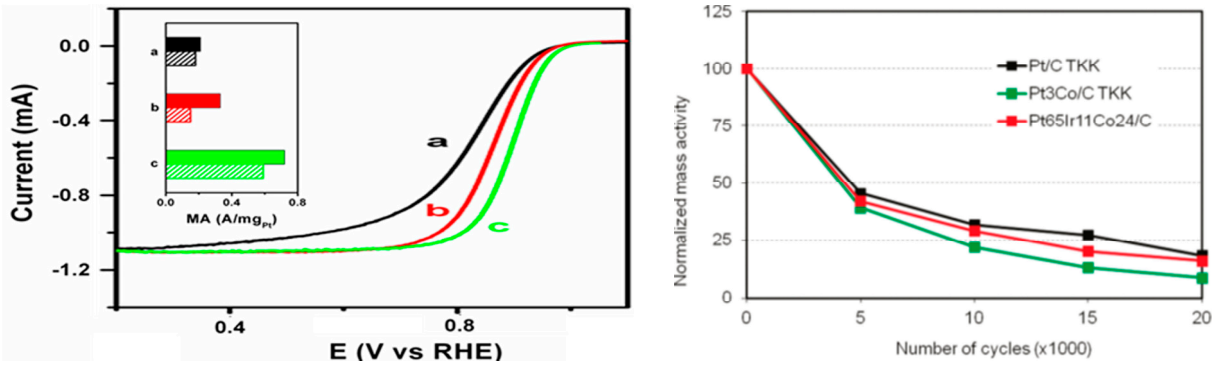

(**A**) (**B**)

Figure 5. Electrocatalytic activities for ORR in O_2-saturated 0.1 M $HClO_4$: (**A**) RDE curves for 400 °C (solid bar) and 800 °C (dash bar) treated catalysts: $Pt_{45}Ir_{55}$/C (**a**), $Pt_{73}Co_{27}$/C (**b**), and $Pt_{25}Ir_{20}Co_{55}$/C (**c**). Insert: Mass activities extracted from RDE curves for the same catalysts. (**B**) Durability plots of normalized mass activities as a function of the number of potential cycles (ranging from 0 to 20,000 cycles) for different catalysts upon potential cycling ((**A**) reproduced from reference [15] with permission. Copyright 2013, American Chemical Society, (**B**) reproduced from reference [34] with permission. Copyright 2012, American Chemical Society).

The durability of the PtIrCo catalysts was also found to show an improvement in comparison with its binary counterparts. This is substantiated by the durability data for the catalysts in the O_2-saturated 0.1 M $HClO_4$ as a function of square-wave potential cycling protocol [34]. Most of the mass activity loss for

all the samples occurred during the initial 5000 cycles (Figure 5B). In comparison with those for the commercial catalysts, the rate of the mass activity loss of $Pt_{65}Ir_{11}Co_{24}$/C was comparable to that of Pt/C and slightly lower than that of Pt_3Co/C. After 20,000 cycles, the mass activity of $Pt_{65}Ir_{11}Co_{24}$/C is found to be higher than that of Pt_3Co/C. The ternary nanoalloy catalyst synthesized by the molecularly-mediated synthesis and thermochemical processing method has durability comparable to that of commercial catalysts upon the severe potential cycling.

4. Summary and Perspectives

In summary, the ability to control the nanoscale alloying structures is essential for understanding the enhanced electrocatalytic activities of Pt or Pd based nanoalloys. It is the unique nanoscale phenomena in terms of atomic-scale alloying, interatomic distances, metal coordination structures, structural/chemical ordering, and phase states that operate synergistically in activating oxygen and maneuvering surface oxygenated species. Understanding this synergy is important for the design of catalysts with high activity with a significantly-reduced use of noble metals [38,39]. In addition to studies aimed at further lowering the noble metal content in the nanoalloy catalysts, future work is needed in the area of theoretical computation and modelling to understand how the structural-catalytic synergy are influenced by the binary or ternary metal composition. This understanding will also guide the development of the ability to enhance the stability of metal components in the nanoalloy catalysts under the electrocatalytic operation conditions. In addition, *in situ* experiments will be very useful to probe the structural evolution processes such as the de-alloying process in the electrolyte and atomic-scale rearrangements leading to changes in size, shape, or surface energy. With recent advents in using synchrotron X-ray based techniques for the study of various catalyst systems, new insights are expected for elucidating the detailed factors controlling the activity and stability of nanoalloy catalysts, which will further advance the endeavor of electrochemical energy conversion and storage.

Acknowledgments

The authors express their gratitude to collaborators who have made contributions to the work described in this article. The research work was supported by the DOE-BES (DE-SC0006877) and NSF (CMMI-1100736).

Author Contributions

Shiyao Shan was the leading author from the initial draft writing to the finalization of the manuscript, during which all authors contributed as a team to the manuscript revisions, the literature reading, and the proof reading. All authors have the expertise in the subject area of the materials described in the manuscript.

Conflicts of Interest

The authors declare no conflict of interest.

References

1. Wu, J.B.; Yang, H. Platinum-Based Oxygen Reduction Electrocatalysts. *Acc. Chem. Res.* **2013**, *46*, 1848–1857.
2. Guo, S.J.; Zhang, S.; Sun, S.H. Tuning Nanoparticle Catalysis for the Oxygen Reduction Reaction. *Angew. Chem. Int. Edit.* **2013**, *52*, 8526–8544.
3. Yu, W.T.; Porosoff, M.D.; Chen, J.G.G. Review of Pt-Based Bimetallic Catalysis: From Model Surfaces to Supported Catalysts. *Chem. Rev.* **2012**, *112*, 5780–5817.
4. Tao, F.; Zhang, S.R.; Nguyen, L.; Zhang, X.Q. Action of bimetallic nanocatalysts under reaction conditions and during catalysis: Evolution of chemistry from high vacuum conditions to reaction conditions. *Chem. Soc. Rev.* **2012**, *41*, 7980–7993.
5. Shi, J.L. On the Synergetic Catalytic Effect in Heterogeneous Nanocomposite Catalysts. *Chem. Rev.* **2013**, *113*, 2139–2181.
6. Wang, C.; Markovic, N.M.; Stamenkovic, V.R. Advanced Platinum Alloy Electrocatalysts for the Oxygen Reduction Reaction. *ACS Catal.* **2012**, *2*, 891–898.
7. Watanabe, M.; Tryk, D.A.; Wakisaka, M.; Yano, H.; Uchida, H. Overview of recent developments in oxygen reduction electrocatalysis. *Electrochim. Acta* **2012**, *84*, 187–201.
8. Cui, C.H.; Yu, S.H. Engineering Interface and Surface of Noble Metal Nanoparticle Nanotubes toward Enhanced Catalytic Activity for Fuel Cell Applications. *Acc. Chem. Res.* **2013**, *46*, 1427–1437.
9. Aiken, J.D.; Finke, R.G. A review of modern transition-metal nanoclusters: Their synthesis, characterization, and applications in catalysis. *J. Mol. Catal. A* **1999**, *145*, 1–44.
10. Qian, H.F.; Zhu, M.Z.; Wu, Z.K.; Jin, R.C. Quantum Sized Gold Nanoclusters with Atomic Precision. *Acc. Chem. Res.* **2012**, *45*, 1470–1479.
11. Hostetler, M.J.; Zhong, C.J.; Yen, B.K.H.; Anderegg, J.; Gross, S.M.; Evans, N.D.; Porter, M.; Murray, R.W. Stable, monolayer-protected metal alloy clusters. *J. Am. Chem. Soc.* **1998**, *120*, 9396–9397.
12. Yang, L.F.; Shan, S.Y.; Loukrakpam, R.; Petkov, V.; Ren, Y.; Wanjala, B.N.; Engelhard, M.H.; Luo, J.; Yin, J.; Chen, Y.S.; *et al*. Role of Support-Nanoalloy Interactions in the Atomic-Scale Structural and Chemical Ordering for Tuning Catalytic Sites. *J. Am. Chem. Soc.* **2012**, *134*, 15048–15060.
13. Petkov, V.; Wanjala, B.N.; Loukrakpam, R.; Luo, J.; Yang, L.F.; Zhong, C.J.; Shastri, S. Pt-Au Alloying at the Nanoscale. *Nano Lett.* **2012**, *12*, 4289–4299.
14. Yin, J.; Shan, S.Y.; Yang, L.F.; Mott, D.; Malis, O.; Petkov, V.; Cai, F.; Ng, M.S.; Luo, J.; Chen, B.H.; *et al*. Gold-Copper Nanoparticles: Nanostructural Evolution and Bifunctional Catalytic Sites. *Chem. Mater.* **2012**, *24*, 4662–4674.
15. Loukrakpam, R.; Shan, S.Y.; Petkov, V.; Yang, L.F.; Luo, J.; Zhong, C.J. Atomic Ordering Enhanced Electrocatalytic Activity of Nanoalloys for Oxygen Reduction Reaction. *J. Phys. Chem. C* **2013**, *117*, 20715–20721.
16. Petkov, V.; Ren, Y.; Shan, S.Y.; Luo, J.; Zhong, C.J. A distinct atomic structure-catalytic activity relationship in 3–10 nm supported Au particles. *Nanoscale* **2014**, *6*, 532–538.

17. Shan, S.Y.; Petkov, V.; Yang, L.F.; Mott, D.; Wanjala, B.N.; Cai, F.; Chen, B.H.; Luo, J.; Zhong, C.J. Oxophilicity and Structural Integrity in Maneuvering Surface Oxygenated Species on Nanoalloys for CO Oxidation. *ACS Catal.* **2013**, *3*, 3075–3085.
18. Galow, T.H.; Drechsler, U.; Hanson, J.A.; Rotello, V.M. Highly reactive heterogeneous Heck and hydrogenation catalysts constructed through "bottom-up" nanoparticle self-assembly. *Chem. Comm.* **2002**, 1076–1077, doi:10.1039/B200334A.
19. Brust, M.; Walker, M.; Bethell, D.; Schiffrin, D.J.; Whyman, R. Synthesis of Thiol-Derivatized Gold Nanoparticles in a 2-Phase Liquid-Liquid System. *J. Chem. Soc. Chem. Comm.* **1994**, *7*, 801–802.
20. Shao, M.H.; Shoemaker, K.; Peles, A.; Kaneko, K.; Protsailo, L. Pt Mono layer on Porous Pd-Cu Alloys as Oxygen Reduction Electrocatalysts. *J. Am. Chem. Soc.* **2010**, *132*, 9253–9255.
21. Schadt, M.J.; Cheung, W.; Luo, J.; Zhong, C.J. Molecularly tuned size selectivity in thermal processing of gold nanoparticles. *Chem. Mater.* **2006**, *18*, 5147–5149.
22. Zhou, Y.; Wang, Z.Y.; Liu, C.J. Perspective on CO oxidation over Pd-based catalysts. *Catal. Sci. Technol*. **2015**, *5*, 69–81.
23. Loukrakpam, R.; Luo, J.; He, T.; Chen, Y.S.; Xu, Z.C.; Njoki, P.N.; Wanjala, B.N.; Fang, B.; Mott, D.; Yin, J.; *et al*. Nanoengineered PtCo and PtNi Catalysts for Oxygen Reduction Reaction: An Assessment of the Structural and Electrocatalytic Properties. *J. Phys. Chem. C* **2011**, *115*, 1682–1694.
24. Prasai, B.; Ren, B.; Shan, S.; Zhao, Y., Cronk, H.; Luo., J.; Zhong, C.J.; Petkov, V. Synthesis-atomic structure-properties relationships in metallic nanoparticles by total scattering experiments and 3D computer simulations: case of Pt-Ru nanoalloy catalysts. *Nanoscale* **2015**, *7*, 8122–8134.
25. Shan, S.Y.; Petkov, V.; Yang, L.F.; Luo, J.; Joseph, P.; Mayzel, D.; Prasai, B.; Wang, L.Y.; Engelhard, M.; Zhong, C.J. Atomic-Structural Synergy for Catalytic CO Oxidation over Palladium-Nickel Nanoalloys. *J. Am. Chem. Soc.* **2014**, *136*, 7140–7151.
26. Yin, J.; Shan, S.Y.; Ng, M.S.; Yang, L.F.; Mott, D.; Fang, W.Q.; Kang, N.; Luo, J.; Zhong, C.J. Catalytic and Electrocatalytic Oxidation of Ethanol over Palladium-Based Nanoalloy Catalysts. *Langmuir* **2013**, *29*, 9249–9258.
27. Wanjala, B.N.; Luo, J.; Loukrakpam, R.; Fang, B.; Mott, D.; Njoki, P.N.; Engelhard, M.; Naslund, H.R.; Wu, J.K.; Wang, L.C.; *et al*. Nanoscale Alloying, Phase-Segregation, and Core-Shell Evolution of Gold-Platinum Nanoparticles and Their Electrocatalytic Effect on Oxygen Reduction Reaction. *Chem. Mater.* **2010**, *22*, 4282–4294.
28. Luo, J.; Wang, L.; Mott, D.; Njoki, P.N.; Lin, Y.; He, T.; Xu, Z.; Wanjana, B.N.; Lim, I.I.S.; Zhong, C.J. Core/Shell Nanoparticles as Electrocatalysts for Fuel Cell Reactions. *Adv. Mater.* **2008**, *20*, 4342–4347.
29. Wanjala, B.N.; Loukrakpam, R.; Luo, J.; Njoki, P.N.; Mott, D.; Zhong, C.J.; Shao, M.H.; Protsailo, L.; Kawamura, T. Thermal Treatment of PtNiCo Electrocatalysts: Effects of Nanoscale Strain and Structure on the Activity and Stability for the Oxygen Reduction Reaction. *J. Phys. Chem. C* **2010**, *114*, 17580–17590.
30. Wanjala, B.N.; Fang, B.; Loukrakpam, R.; Chen, Y.S.; Engelhard, M.; Luo, J.; Yin, J.; Yang, L.F.; Shan, S.Y.; Zhong, C.J. Role of Metal Coordination Structures in Enhancement of Electrocatalytic Activity of Ternary Nanoalloys for Oxygen Reduction Reaction. *ACS Catal.* **2012**, *2*, 795–806.

31. Wanjala, B.N.; Fang, B.; Shan, S.Y.; Petkov, V.; Zhu, P.Y.; Loukrakpam, R.; Chen, Y.S.; Luo, J.; Yin, J.; Yang, L.F.; *et al*. Design of Ternary Nanoalloy Catalysts: Effect of Nanoscale Alloying and Structural Perfection on Electrocatalytic Enhancement. *Chem. Mater.* **2012**, *24*, 4283–4293.
32. Wanjala, B.N.; Fang, B.; Luo, J.; Chen, Y.S.; Yin, J.; Engehard, M.H.; Loukrakpam, R.; Zhong, C.J. Correlation between Atomic Coordination Structure and Enhanced Electrocatalytic Activity for Trimetallic Alloy Catalysts. *J. Am. Chem. Soc.* **2011**, *133*, 12714–12727.
33. Chen, G.X.; Zhao, Y.; Fu, G.; Duchesne, P.N.; Gu, L.; Zheng, Y.P.; Weng, X.F.; Chen, M.S.; Zhang, P.; Pao, C.W.; *et al*. Interfacial Effects in Iron-Nickel Hydroxide-Platinum Nanoparticles Enhance Catalytic Oxidation. *Science* **2014**, *344*, 495–499.
34. Loukrakpam, R.; Wanjala, B.N.; Yin, J.; Fang, B.; Luo, J.; Shao, M.H.; Protsailo, L.; Kawamura, T.; Chen, Y.S.; Petkov, V.; *et al*. Structural and Electrocatalytic Properties of Nanoengineered PtIrCo Catalysts for Oxygen Reduction Reaction. *ACS Catal.* **2011**, *1*, 562.
35. Luo, J.; Han, L.; Kariuki, N.N.; Wang, L.Y.; Mott, D.; Zhong, C.J.; He, T. Synthesis and characterization of monolayer-capped PtVFe nanoparticles with controllable sizes and composition. *Chem Mater.* **2005**, *17*, 5282–5290.
36. Luo, J.; Kariuki, N.; Han, L.; Wang, L.Y.; Zhong, C.J.; He, T. Preparation and characterization of carbon-supported PtVFe electrocatalysts. *Electrochim. Acta* **2006**, *51*, 4821–4827.
37. Zhang, J.; Sasaki, K.; Sutter, E.; Adzic, R.R. Stabilization of platinum oxygen-reduction electrocatalysts using gold clusters. *Science* **2007**, *315*, 220–222.
38. Anderson, R.M.; Yancey, D.F.; Zhang, L.; Chill, S.T.; Henkelman, G.; Crooks, R.M. A Theoretical and Experimental Approach for Correlating Nanoparticle Structure and Electrocatalytic Activity. *Acc. Chem. Res.* **2015**, *48*, 1351–1357.
39. Nie, Y.; Li, L.; Wei, Z.D. Recent advancements in Pt and Pt-free catalysts for oxygen reduction reaction. *Chem. Soc. Rev.* **2015**, *44*, 2168–2201.